Journal of Crystal Growth 378 (2013) 291–294

Contents lists available at SciVerse ScienceDirect

Journal of Crystal Growth

journal homepage: www.elsevier.com/locate/jcrysgro

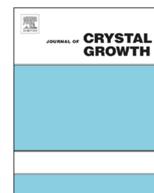

Growth of cubic GaN on 3C–SiC/Si (001) nanostructures

R.M. Kemper [a,*], L. Hiller [b], T. Stauden [b], J. Pezoldt [b], K. Duschik [c], T. Niendorf [c], H.J. Maier [c], D. Meertens [d], K. Tillmann [d], D.J. As [a], J.K.N. Lindner [a]

[a] University of Paderborn, Department of Physics, Warburger Str. 100, 33098 Paderborn, Germany
[b] FG Nanotechnologie, Institut für Mikro- und Nanotechnologien MacroNano®, Technische Universität Ilmenau, Postfach 100565, 98684 Ilmenau, Germany
[c] University of Paderborn, Lehrstuhl für Werkstoffkunde (Materials Science), Pohlweg 47-49, 33098 Paderborn, Germany
[d] Ernst-Ruska Center for Microscopy and Spectroscopy with Electrons, Forschungszentrum Jülich, 52425 Jülich, Germany

ARTICLE INFO

Available online 16 October 2012

Keywords:
A1. Nanostructures
A1. Planar defects
A3. Molecular beam epitaxy
A3. Selective epitaxy
B1. Nitrides

ABSTRACT

We report on the molecular beam epitaxy growth of cubic GaN on 3C–SiC (001) nanostructures. Transmission electron microscopy (TEM) studies show phase-pure cubic GaN crystals with a low defect density on top of the post shaped 3C–SiC nanostructures and GaN grown on their sidewalls, which is dominated by {111} planar defects. The nanostructures, aligned parallel and perpendicular to the [110] directions of the substrate, are located in anti-phase domains of the 3C–SiC/Si (001) substrate. These anti-phase domains strongly influence the optimum growth of GaN layers in these regions. TEM measurements demonstrate a different stacking fault density in the cubic GaN epilayer in these areas.
© 2012 Elsevier B.V. All rights reserved.

1. Introduction

Group III-nitrides, especially GaN, are well-suited semiconductors for electronic and optoelectronic devices like highly efficient laser diodes and transistors [1–3]. In state-of-the-art devices the wurtzite phase of GaN is used, which – however – due to its crystal symmetry exhibits spontaneous and piezoelectric polarization fields along the *c*-axis leading to performance degrading effects. In contrast the meta-stable cubic phase of GaN (c-GaN) is free of these internal fields due to its non-polar nature. Hence there is a growing interest in the growth of the non-polar c-GaN.

One of the key issues in group III-nitride growth is the improvement of the structural quality, because defects like dislocations limit the device performance. Many of these defects are due to the lattice mismatch with the substrate. For c-GaN, 3C–SiC is the preferred substrate, exhibiting a lattice misfit of 3.5%. This is meant to be the main reason for the present high dislocation density of 10^9–10^{10} cm^{-2} in c-GaN. One possibility to eliminate these misfit dislocations is the reduction of the growth area [4,5]. In recent work it was shown that another source of defects is the presence of two types of anti-phase domains in the 3C–SiC/Si substrate sharing equal parts of the growth surface [6]. Our aim is to grow defect reduced c-GaN on 3C–SiC nanostructures. Here, we study the growth of GaN on post shaped nanostructures and analyze the influence of substrate domains on the defect structure.

2. Experiment

Cubic GaN was grown by plasma-assisted molecular beam epitaxy (MBE) on nanopatterned 3C–SiC/Si (001) surfaces exhibiting anti-phase domains. The substrate consists of a 12 μm thick 3C–SiC (001) layer, which was deposited by low-pressure chemical vapor deposition on 500 μm Si (001) [7].

Patterning of the 3C–SiC (001) surface is achieved by electron beam lithography and a subsequent reactive ion etching process [8]. Fig. 1 displays a side view scanning electron microscopy (SEM) image of the 3C–SiC (001) surface with post shaped nanostructures. Arrays of 5×5 nanostructures are repeated several times on the substrate surface with etched down spaces in between. The posts have top edges with a length of about 500 nm, a height of about 700 nm and are aligned parallel and perpendicular to the [110] direction of the substrate. These arrays and the etched down 3C–SiC surface in between were overgrown with 400 nm GaN under 1 monolayer Ga coverage on the surface and a growth temperature of 740 °C [9]. The growth process was monitored by in-situ reflection high energy electron diffraction (RHEED). After growth the c-GaN epilayer was characterized by electron backscatter diffraction (EBSD) and the selective-area-grown GaN was analyzed by cross-section transmission electron microscopy (TEM). To this end the post structures were prepared using a focused ion beam. The TEM lamellas were cut from different post arrays parallel to the [110] direction.

* Corresponding author. Tel.: +4952 5160 5830; fax: +4952 5160 5843.
E-mail address: rkemper@mail.uni-paderborn.de (R.M. Kemper).

0022-0248/$ - see front matter © 2012 Elsevier B.V. All rights reserved.
http://dx.doi.org/10.1016/j.jcrysgro.2012.10.011

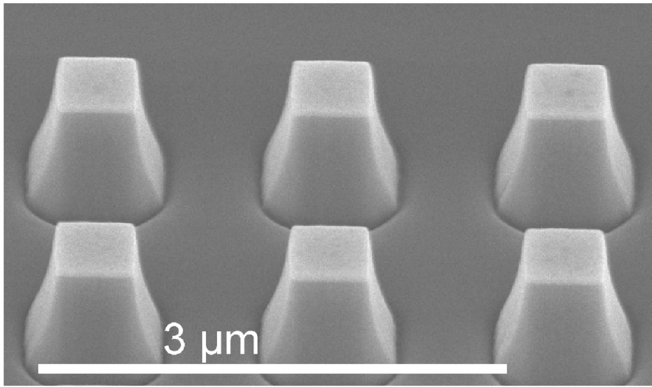

Fig. 1. Side view of SEM image of the 3C–SiC (001) surface with post shaped SiC nanostructures.

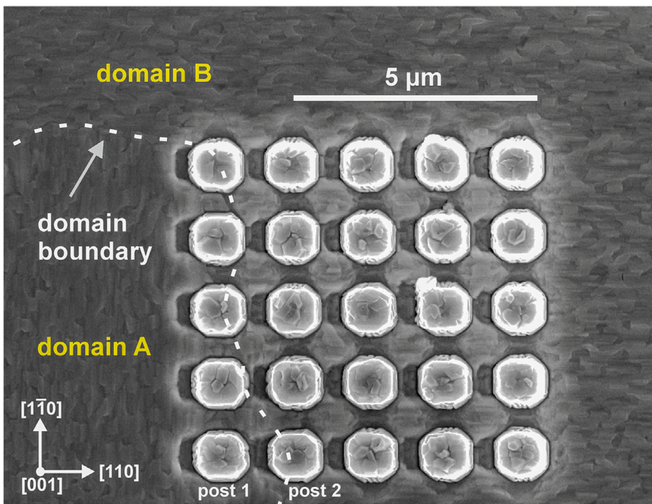

Fig. 2. Top view of SEM image of a nanostructure array overgrown with 400 nm c-GaN. The c-GaN surface exhibits surface striations in two perpendicular orientations parallel to [110] and [1$\bar{1}$0], which are considered to belong to be APDs with a boundary in between.

3. Results and discussion

3.1. Cubic GaN grown on 3C–SiC (001) posts

Former studies [6] have shown that the c-GaN surfaces grown on 3C–SiC/Si (001) substrates exhibit surface striations in two perpendicular orientations parallel to the [110] and [1$\bar{1}$0] directions of the substrate. Corresponding surface regions are considered to belong to two anti-phase domains (APDs) with a boundary in between. The structural quality within these APDs is not equal which can be attributed to an anisotropic growth of Ga- and N-terminated {111} planes. In addition the defect formation within the ADPs is different and can be allocated to the crystal direction [6].

Fig. 2 shows a SEM top view image of post shaped 3C–SiC (001) nanostructures overgrown with 400 nm c-GaN. The edge length of the post structures is increased after GaN overgrowth from about 500 nm to about 1 µm. Furthermore there are darker areas in between neighboring posts, indicating deepenings in the GaN layer. They arise probably due to shadowing in particular when the rotation of the sample holder is stopped during MBE growth for RHEED inspection of the growth surface.

A domain boundary, separating two domains with their characteristic orientation of surface striations, is clearly visible. In domain A the surface striations are perpendicular to the [110] direction and in domain B the striation orientation is parallel to the [110] direction. The array of posts is located in both types of domains. In the bottom row, the domain boundary passes through post 2 (see Fig. 2).

To have a closer look to the selective-area-grown GaN on the post structures, Fig. 3(a) displays a cross-sectional TEM bright-field micrograph of an individual 3C–SiC (001) post overgrown with 400 nm cubic GaN taken along the [110] zone axis. The GaN surface is covered with a Pt protection film (dark in Fig. 3(a)) necessary in the TEM lamella preparation process. The image shows that the GaN grows on the top of the 3C–SiC post and on its sidewalls. Since the TEM lamella was taken through the sidewall of the post and not through the center (Fig. 3(b)), the GaN is visible on three sidewalls of the post. This leads to the strongly varying contrasts within the upper part of the SiC post, since here almost defect free crystal lattice of the SiC post is superimposed with the defect rich GaN growing on the flanks of posts. The GaN on the top of the post grows in individual crystals. It should be emphasized that the part of the GaN film displayed in Fig. 3(a) is located at the edge of the GaN top layer. The homogeneous

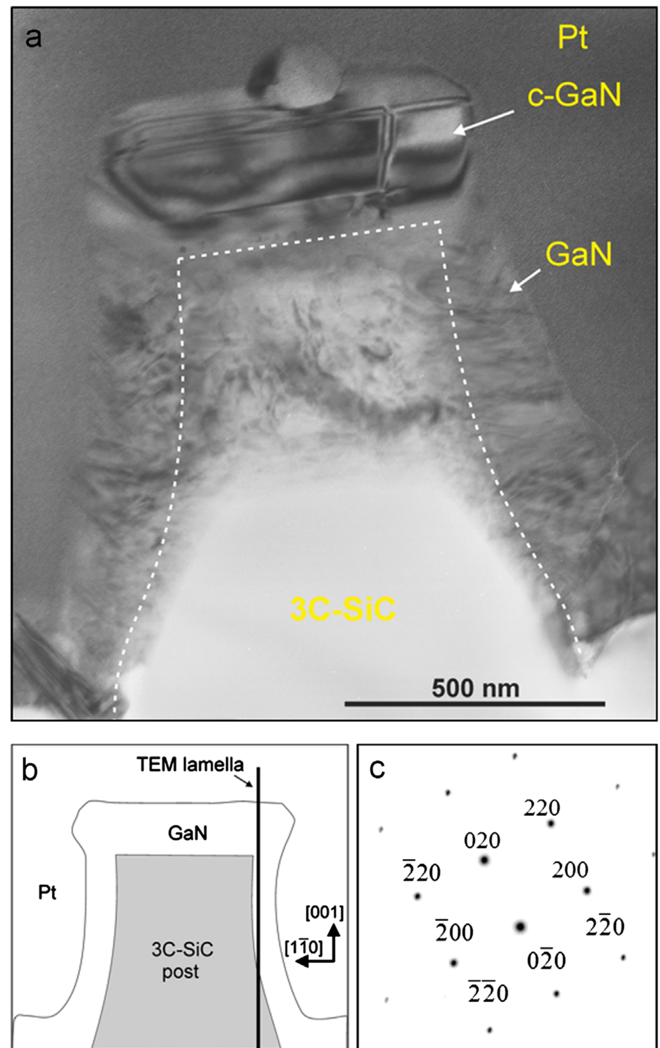

Fig. 3. (a) Cross-sectional TEM image of an individual 3C–SiC post overgrown with 400 nm cubic GaN taken along the [110] zone axis. (b) A schematic cross-section view through the center of a typically overgrown SiC post parallel to the [1$\bar{1}$0] direction. The TEM lamella cuts through the sidewall of the post perpendicular to the [1$\bar{1}$0] direction. (c) Selected area diffraction pattern (contrast inverted) taken from the middle cubic GaN island in (a) along the [001] cubic GaN zone axis with the main reflections indexed.

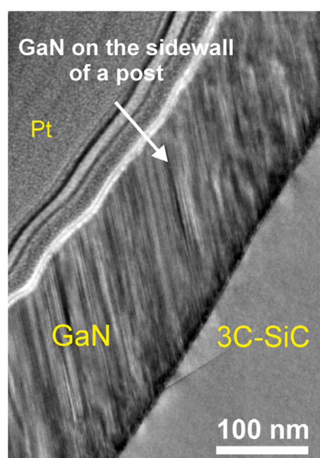

Fig. 4. TEM image of GaN grown on a SiC post sidewall taken along the [110] zone axis. The GaN growth is dominated by {111} planar defects. The parallel lines along the GaN surface are thickness fringes of the TEM lamella.

contrasts within this part of the GaN film indicates a very low defect density of the GaN growing on top of the SiC post. There is only one dislocation like defect running vertically in the GaN top bit. The corresponding selected area diffraction (SAD) pattern taken from the central GaN area on top of the post in (a) is shown in (c). The diffraction pattern can be completely assigned to the lattice of cubic GaN with the [001] zone axis oriented parallel to the electron beam. The SAD pattern contains no further reflections indicating a crystal with a pure cubic phase. These are the first steps towards defect reduced cubic GaN grown via MBE on a dimensionally limited 3C–SiC (001) growth area. However, we also found a small misaligned GaN crystal centered on top of the epitaxial GaN film, not contributing to the SAD pattern shown.

Fig. 4 shows a TEM image of GaN grown on a SiC post sidewall taken along the [110] zone axis under higher magnification. The GaN growth is dominated by {111} planar defects. One reason for this could be the sidewall surface roughness resulting from the etching process during substrate patterning. Another reason is probably the deviation from an ideal 90° slope of the flanks. The GaN layer thickness on the sidewalls is smaller than on top of the post. Hence there is a lower GaN growth rate on the sidewalls than on top of the 3C–SiC post.

3.2. Defects in cubic GaN anti-phase domains

To identify the two types of domains an EBSD phase map taken from the thin GaN epilayer surface next to the array of posts in Fig. 2 is shown in Fig. 5. The EBSD phase map is based on Kikuchi diffraction patterns consisting of bands assigned to the crystal planes of c-GaN. Fig. 5 displays regions colored in dark and light red sharing equal parts of the surface. The color gradation corresponds to the "fit" parameter which defines the average angular deviation between the detected Kikuchi-diffraction pattern and the theoretical diffraction pattern. On average, bright red and dark red regions differ in fit parameter by about 0.5° with respect to each other. They represent the two APDs sharing nearly equal parts of the surface.

The comparison of the EBSD orientation map with a SEM image of the EBSD measurement area (not shown here) indicates a perfect agreement between the morphological (SEM) and orientational domain patterns (EBSD) [6]. Domains with striations parallel [110] are shown in light red and domains with striations perpendicular to the [110] direction are colored in dark red in Fig. 5. In this way domain A and B in Fig. 2 can clearly be

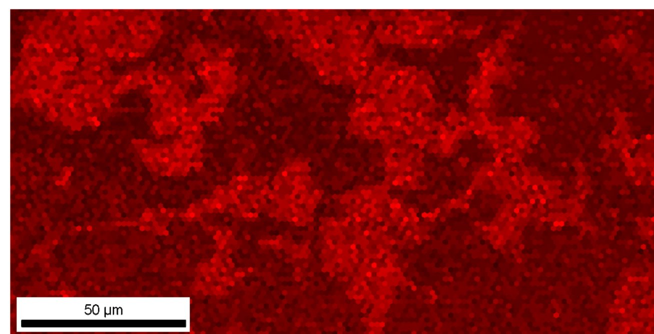

Fig. 5. Section of an EBSD phase map with superimposed fit parameter of a 400 nm thick cubic GaN surface showing regions of dark and light red. (For interpretation of the references to color in this figure legend, the reader is referred to the web version of this article.)

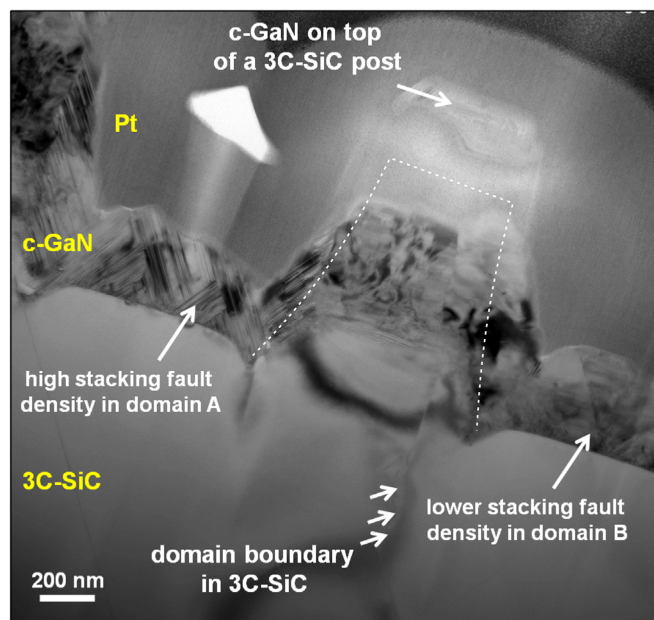

Fig. 6. Cross-sectional TEM image of an individual 3C–SiC post overgrown with 400 nm cubic GaN taken along the [110] zone axis. A domain boundary coming from the 3C–SiC substrate runs through the 3C–SiC post (post 2 in Fig. 2). Hence the cubic GaN grown on the left and the right side of the post belong to adjoining anti-phase domains (domains A and B in Fig. 2). The stacking fault density on the left side of the post is significantly higher than on the right side.

identified. Domain A belongs to a domain which is colored in dark red and domain B is identified as a light red domain.

Fig. 6 shows a cross-sectional TEM image of post 2 taken from the bottom row of the post array in Fig. 2. The bright-field image was taken along the [110] zone axis where the typical {111} planar defects appear edge-on and lead to lineshaped contrasts. Next to post 2 the GaN epilayer grown between the posts is visible, together with post 1 on the left. Again, a low defect density GaN top film is observable on top of the SiC post, which due to the non-central FIB cut appears to be disconnected from the SiC post. The GaN grown on the SiC post sidewalls is dominated by {111} planar defects.

A domain boundary crossing the 3C–SiC substrate runs through the SiC post towards the GaN top surface. The same boundary is visible in the SEM image of the GaN surface in Fig. 2 where it runs through post 2 of the bottom row of posts. Hence the c-GaN grown on the left and the right side of the post belong to adjoining anti-phase domains, called domain A and B,

respectively, in Fig. 2. It is obvious that the stacking fault density left to the domain boundary, i.e. in domain A is significantly higher than in domain B. Therefore it is evident that at the same growth conditions, the two different domains in the SiC substrate lead to largely different c-GaN crystal qualities. We assume a relationship between the different crystal qualities in the domains and the varying fit parameter of the EBSD measurements. Previous EBSD studies [6] have shown that in thick GaN epilayers ($>1\ \mu m$) one type of the domains contains a higher fraction of hexagonal inclusions than the other.

It is conceivable that in the thin layers, shown here, a higher stacking fault density leads to barely visible changes in the Kikuchi patterns, expressed by a different fit parameter. These relationships are the subject of further studies. The connection between both measurement methods would allow for the preselection of the domains in a thin c-GaN layer with a non-destructive method like EBSD.

4. Conclusion

In this work, first steps towards the MBE growth of defect reduced c-GaN on a dimensionally limited 3C–SiC (001) growth area are demonstrated. The overgrown 3C–SiC (001) nanostructures are post shaped and aligned parallel and perpendicular to the [110] directions of the substrate. On top of the nano-sized 3C–SiC posts nearly defect-free phase-pure c-GaN with excellent structural properties is grown. On the sidewalls of these posts, however, the GaN layer contains a high density of {111} planar defects. For c-GaN grown in the intermediate area between the 3C–SiC posts the stacking fault density in adjoining anti-phase domains is markedly different, with the domain boundary clearly separating regions of low and high planar defect densities. Such an observation is not seen on top of the posts up to now, however for more details TEM investigations have to be performed to clarify this conclusion.

Acknowledgment

The work at Paderborn was financially supported by the German Science Foundation (As (107/4-1)).

References

[1] S. Nakamura, I. Mukai, M. Senok, Applied Physics Letters 64 (1994) 1687.
[2] S. Rajan, P. Waltereit, C. Poblenz, S.J. Heikman, D.S. Green, J.S. Speck, U.K. Mishra, IEEE Electron Device Letters 25 (2004) 247.
[3] H. Machhadani, M. Tchernycheva, S. Sakr, L. Rigutti, R. Colombelli, E. Warde, C. Mietze, D.J. As, F.H. Julien, Physical Review B 83 (2011) 075313.
[4] E.A. Fitzgerald, G.P. Watson, R.E. Proano, D.G. Ast, Journal of Applied Physics 65 (1989) 2220.
[5] D. Zubia, S.D. Hersee, Journal of Applied Physics 85 (1999) 6492.
[6] R.M. Kemper, T. Schupp, M. Häberlen, T. Niendorf, H.-J. Maier, A. Dempewolf, F. Bertram, J. Christen, R. Kirste, A. Hoffmann, J. Lindner, D.J. As, Journal of Applied Physics 110 (2011) 123512.
[7] T. Chassagne, A. Leycuras, C. Balloud, P. Arcade, H. Peyre, S. Juillaguet, Materials Science Forum 457–460 (2004) 273–276.
[8] L. Hiller, T. Stauden, R.M. Kemper, J.K.N. Lindner, D.J. As, J. Pezoldt, Proceedings of Materials Science Forum 717–720 (2012) 901.
[9] J. Schörmann, S. Potthast, D.J. As, K. Lischka, Applied Physics Letters 90 (2009) 041918.